A main sequence for quasars

Paola Marziani[1]

in collaboration with

J. W. Sulentic[2], D. Dultzin[3], A. Negrete[3], A. del Olmo[2], M. A. Martínez-Carballo[2], G. M. Stirpe[4], M. D'Onofrio[5], J. Perea[2]

[1]INAF - Osservatorio Astronomico di Padova, Padova, Italia
[2]Instituto de Astrofísica de Andalucía (CSIC), Granada, España
[3]Instituto de Astronomía, UNAM, México, D.F., México
[4]INAF - Osservatorio Astronomico di Bologna, Bologna, Italia
[5]Dipartimento di Fisica ed Astronomia "Galileo Galilei", U. di Padova, Padova, Italia

GN12
XII Congresso Nazionale sui Nuclei Galattici Attivi

September 26–29, 2016 — Napoli, Italia

Luminous Seyfert 1 and quasars (i.e., of **type-1 AGN**; log L>43) are mainly unobscured accretors, offering an unimpeded view of the broad line emitting region (BLR).

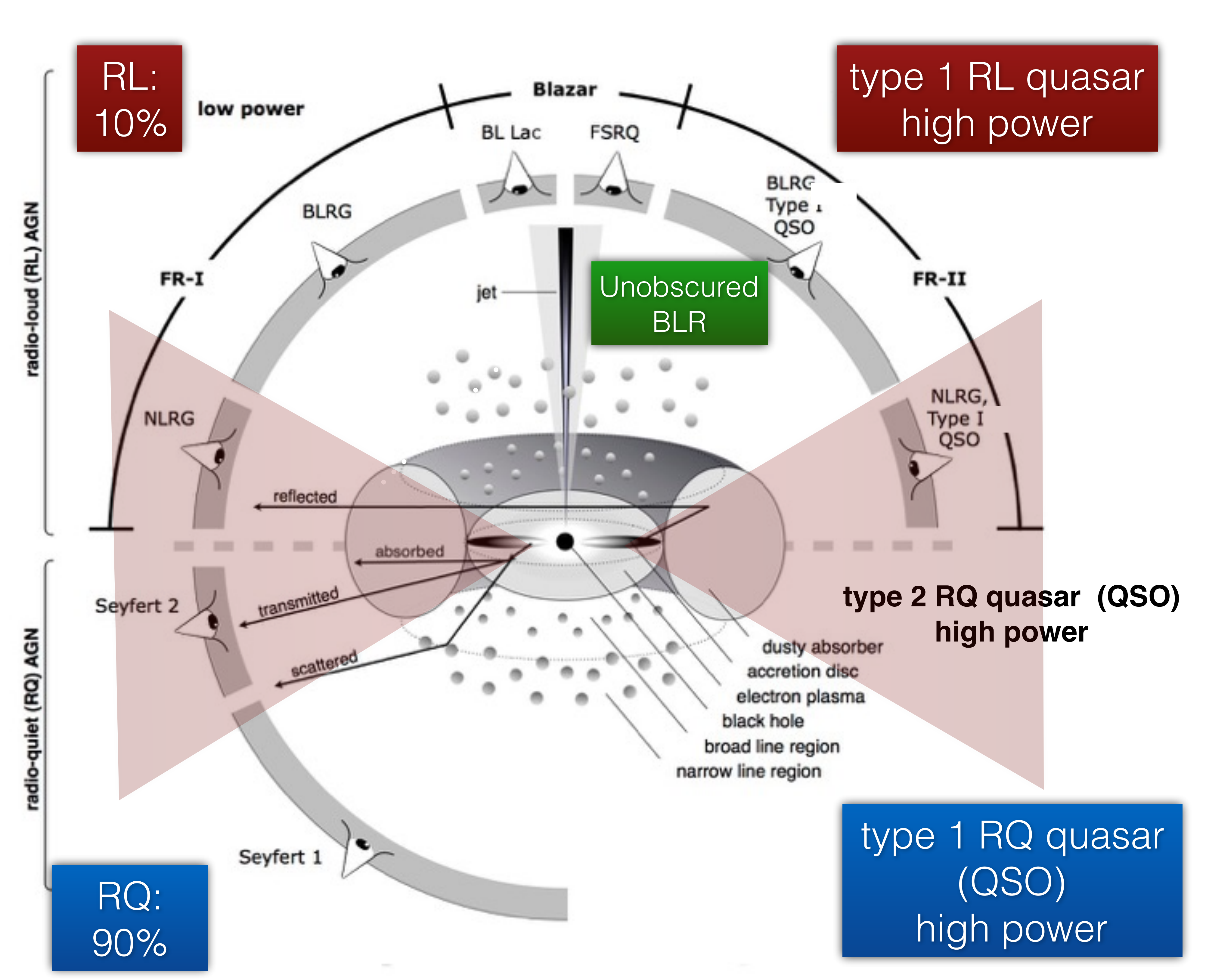

Adapted from
Beckmann & Shrader 2013

Prediction of unification schemes on spectral properties of type-1 AGN

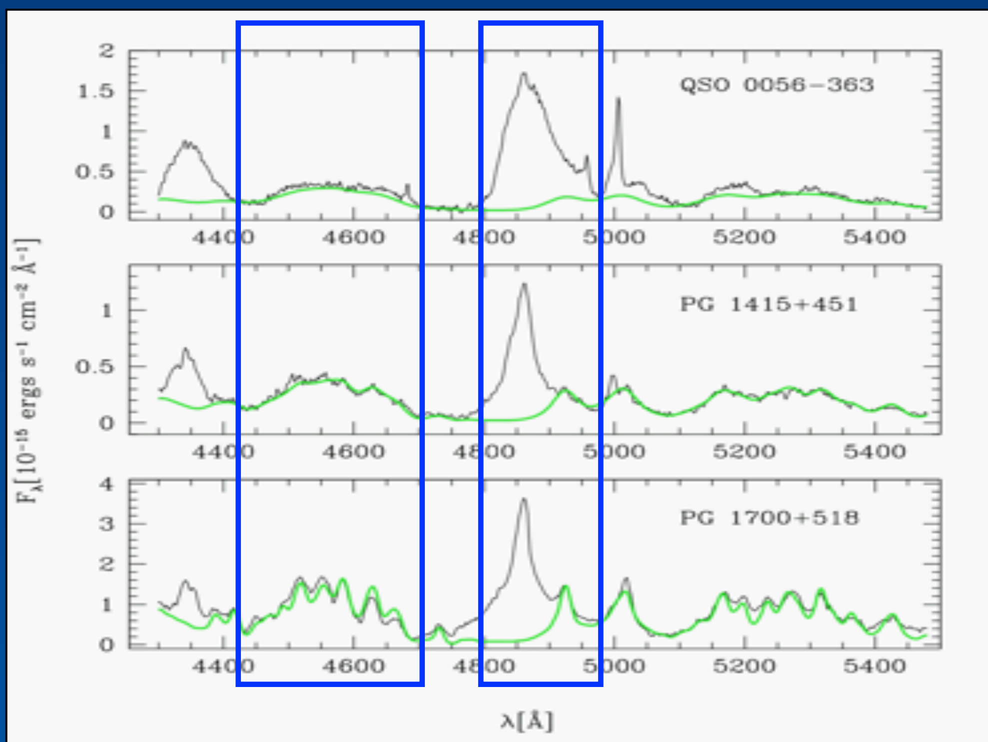

$$R_{\rm FeII} = \frac{I({\rm FeII}\lambda4570)}{I(H\beta)} \approx \frac{W({\rm FeII}\lambda4570)}{W(H\beta)}$$

$$FWHM(H\beta)$$

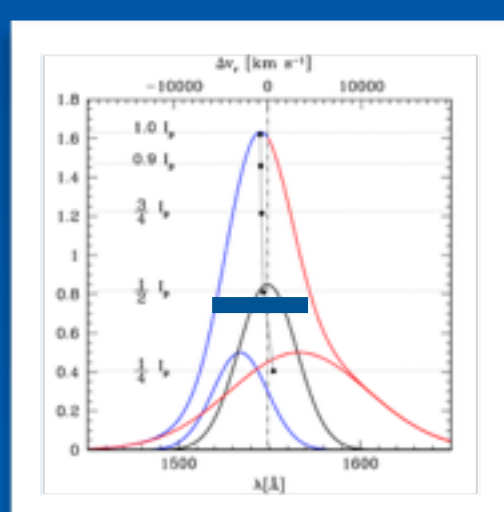

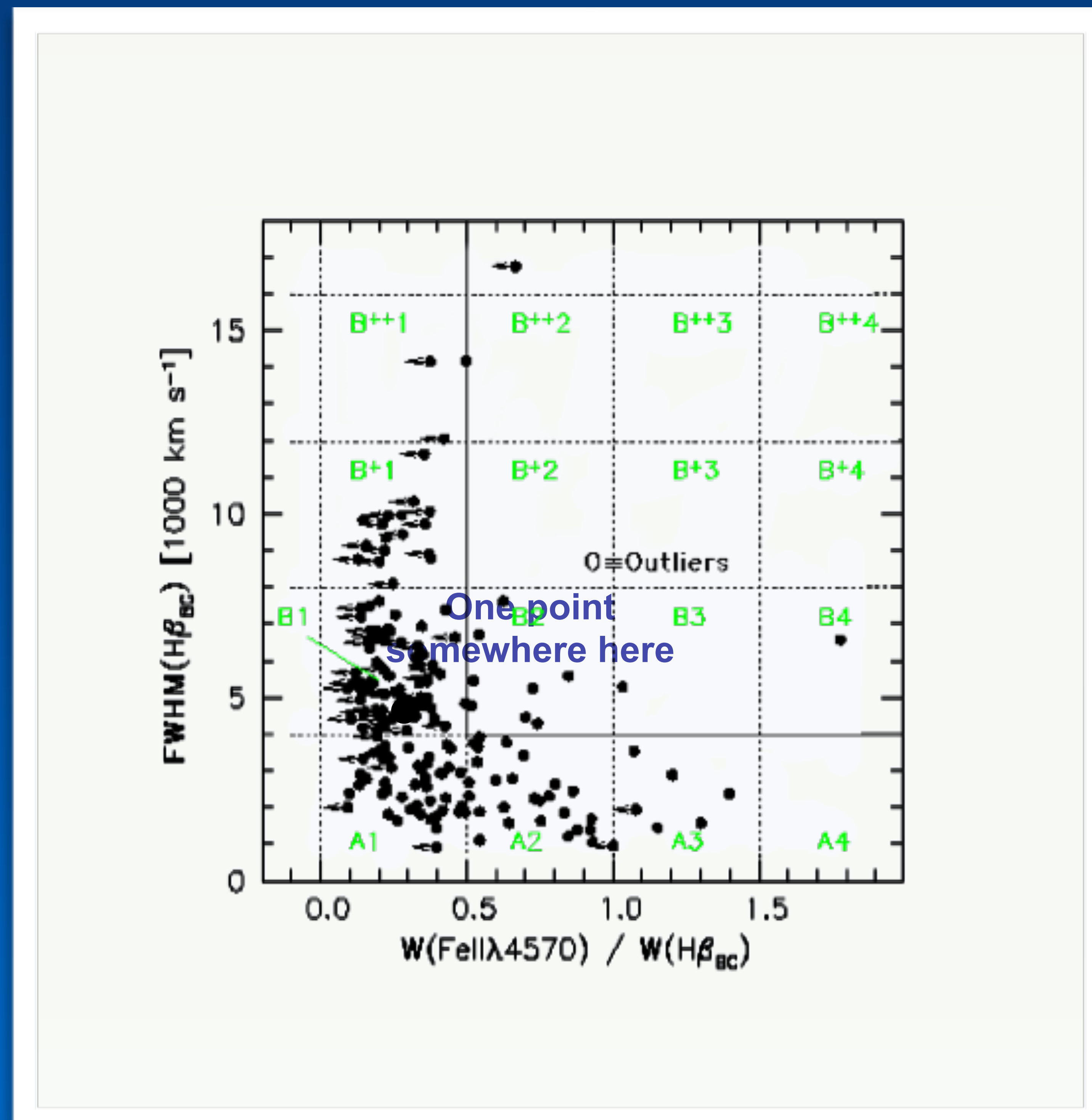

The quasar Eigenvector 1: a main sequence for quasars

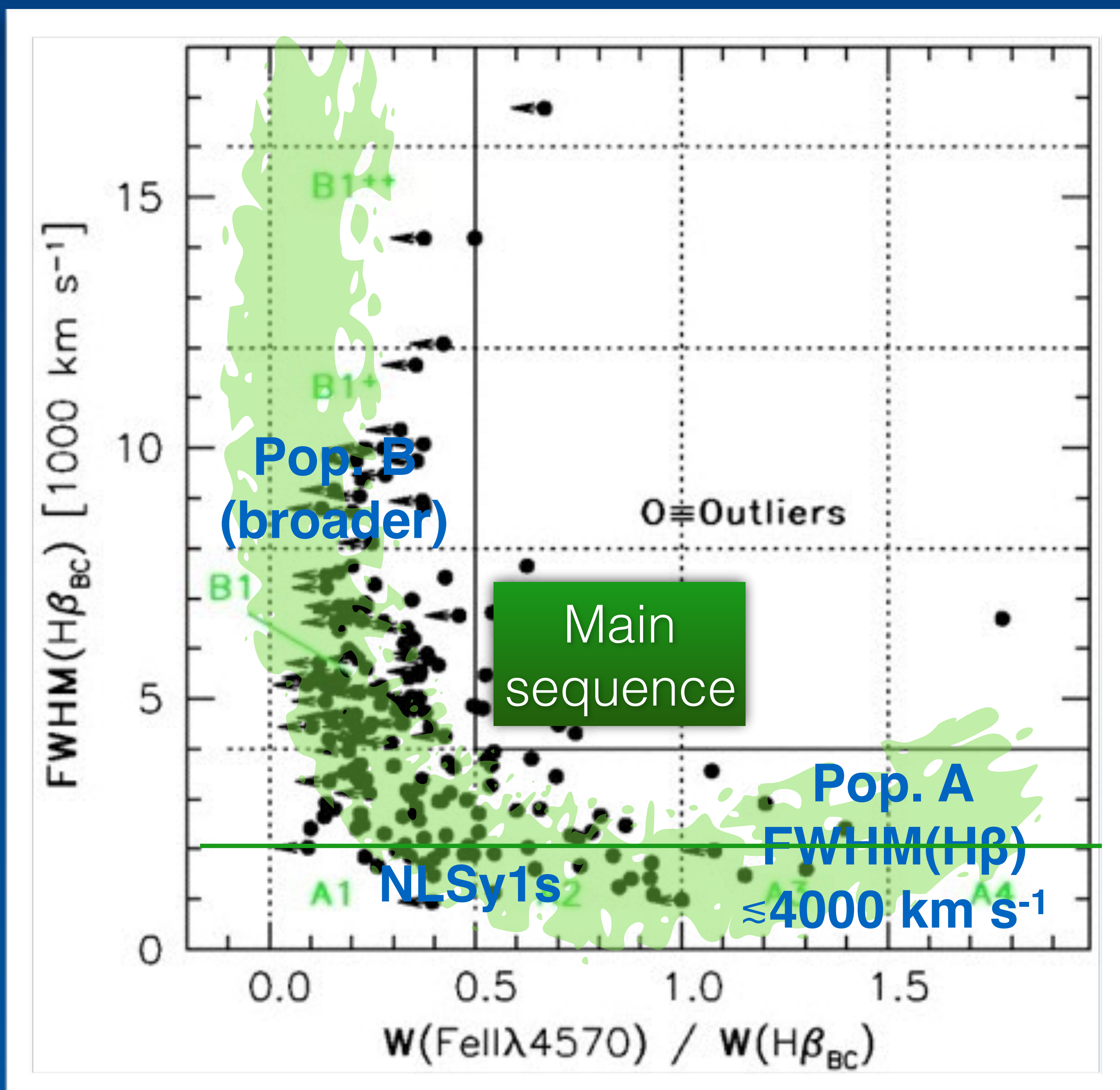

Sulentic et al. 2002 ($z < 1$, log L < 47 [erg/s])

Principal Component Analysis (PCA): n×m matrix with m parameters for n objects finds axes in m-dimensional space that maximize projection onto versors.

Eigenvector 1: Originally defined by a PCA of PG quasars (Boroson & Green 1992), and associated with an anti-correlation between strength of FeIIλ4570 (or [OIII] 5007 peak intensity) and width of Hβ.

The E1 main sequence (MS) allows for the definition of spectral types.

Since 1992, E1 has been found in increasingly larger samples with multifrequency parameters.

MS Correlates: The Hβ profile

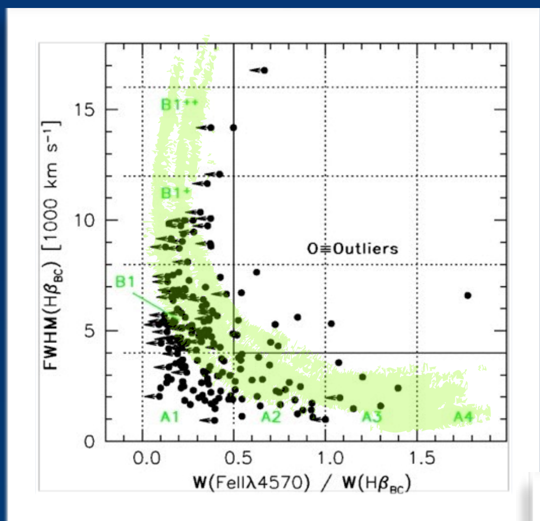

Pop. A.: "Lorentzian" Hβ profile, symmetric, unshifted;
Pop. B.: Double Gaussian (broad + very broad component Hβ$_{BC}$+Hβ$_{VBC}$), most often redward asymmetric

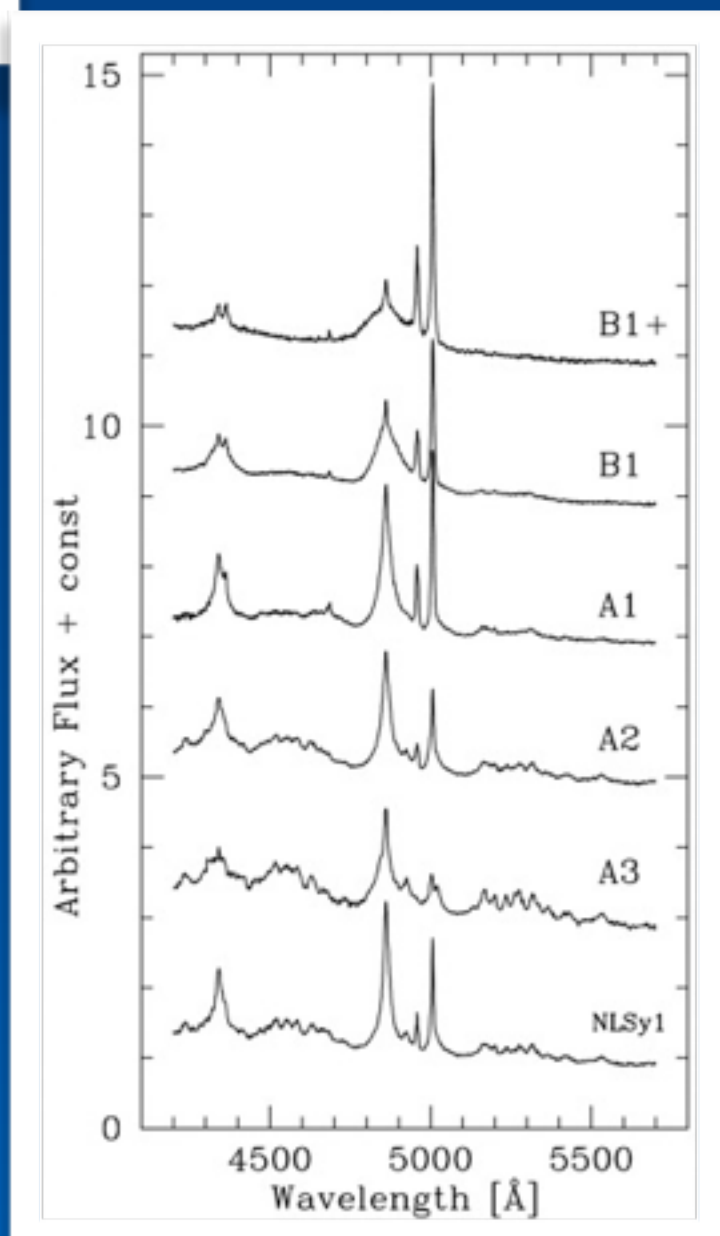

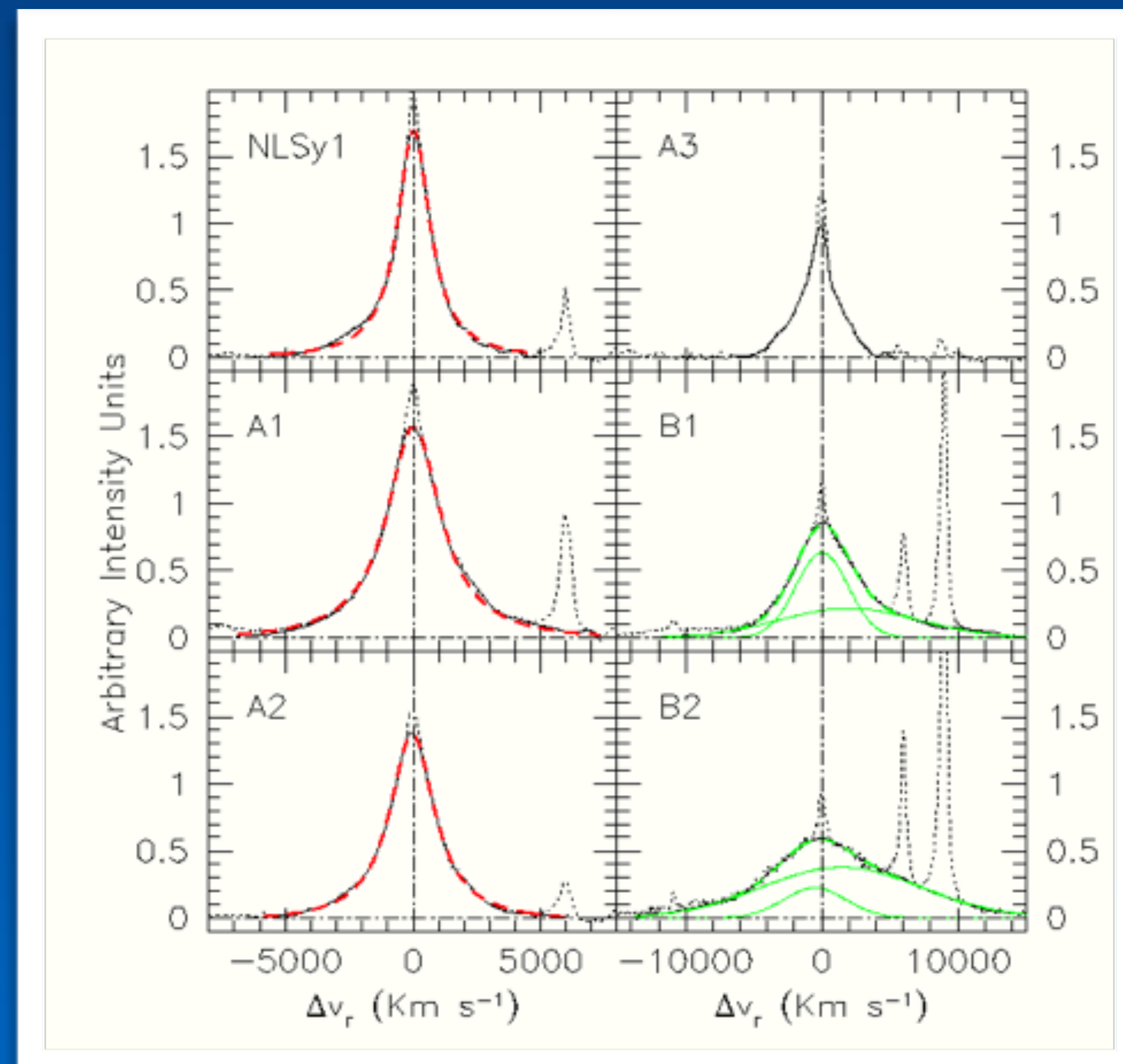

Sulentic et al. 2002 ($z < 1$, log L < 47 [erg/s])

MS correlates: UV lines

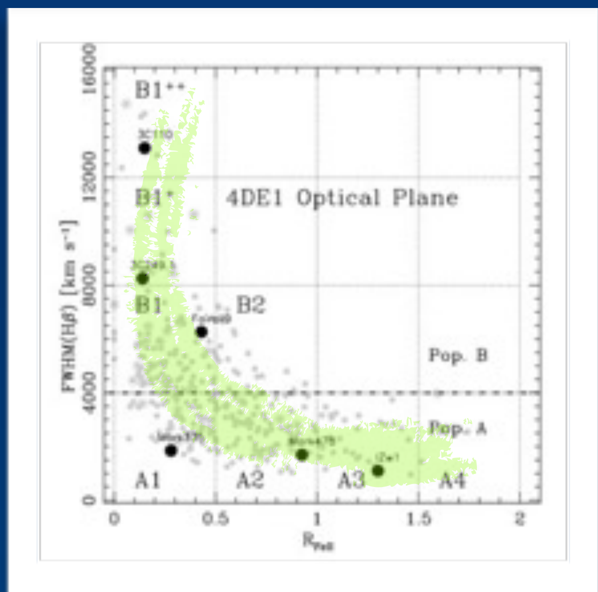

($B1^{++}$ → A4) NVλ1240⬆ AlIIIλ1860⬆ CIII]λ1909⬇

NIII]1750 ⬆ CIVλ1549 ⬇

Metallicity- and density-sensitive emission line ratios imply growth of density and metallicity toward A4

n: AlIIIλ1860/ SiIII]λ1892

SiIII]λ1892/ CIII]λ1909

$Z/Z_{\odot}$ NVλ1240/ CIVλ1549

NVλ1240/ Heλ1640

Bachev et al. 2004; Negrete et al. 2012 HST/FOS composite spectra of quasars at *z*<0.7; cf. Sulentic et al. 2015

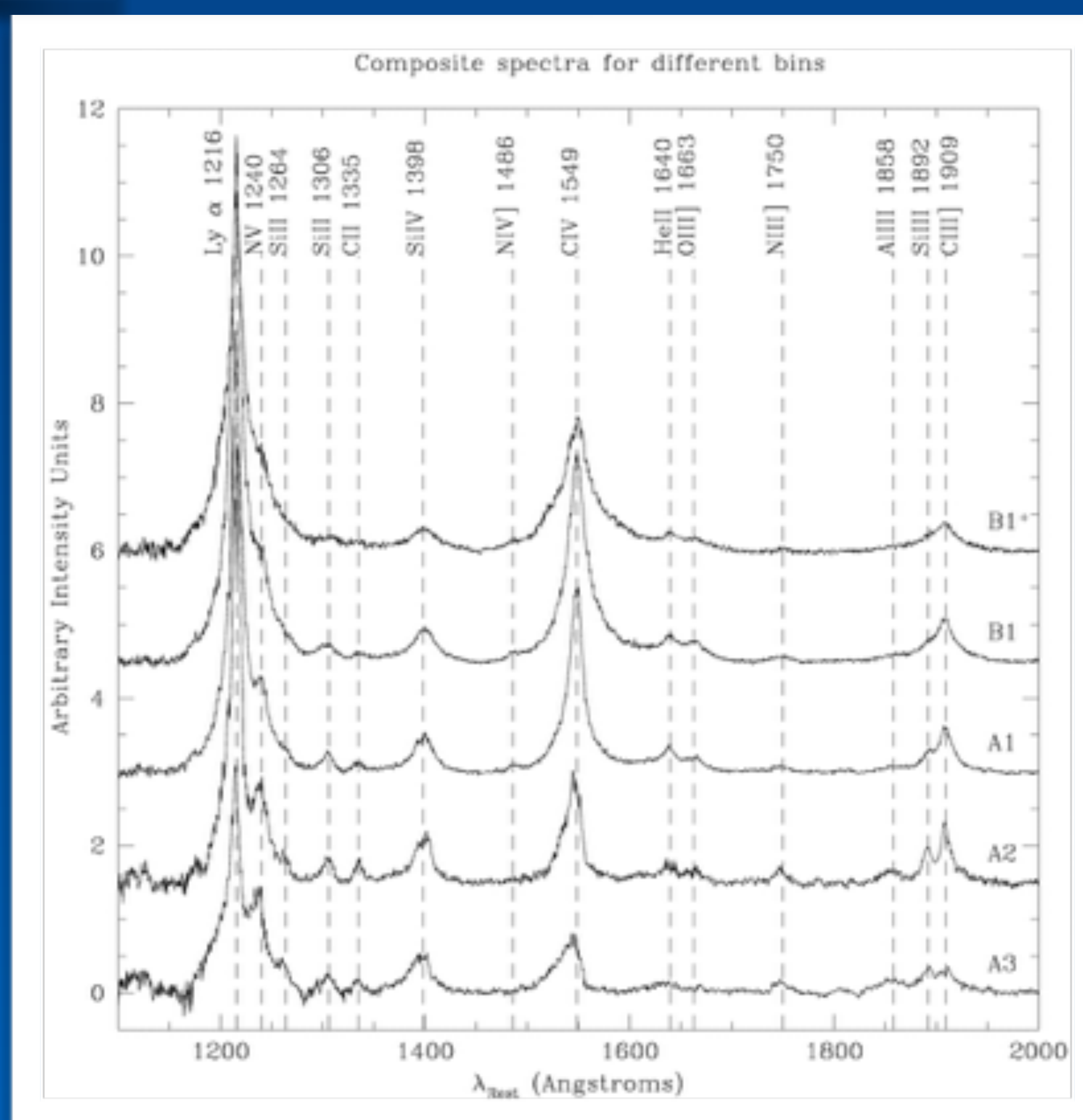

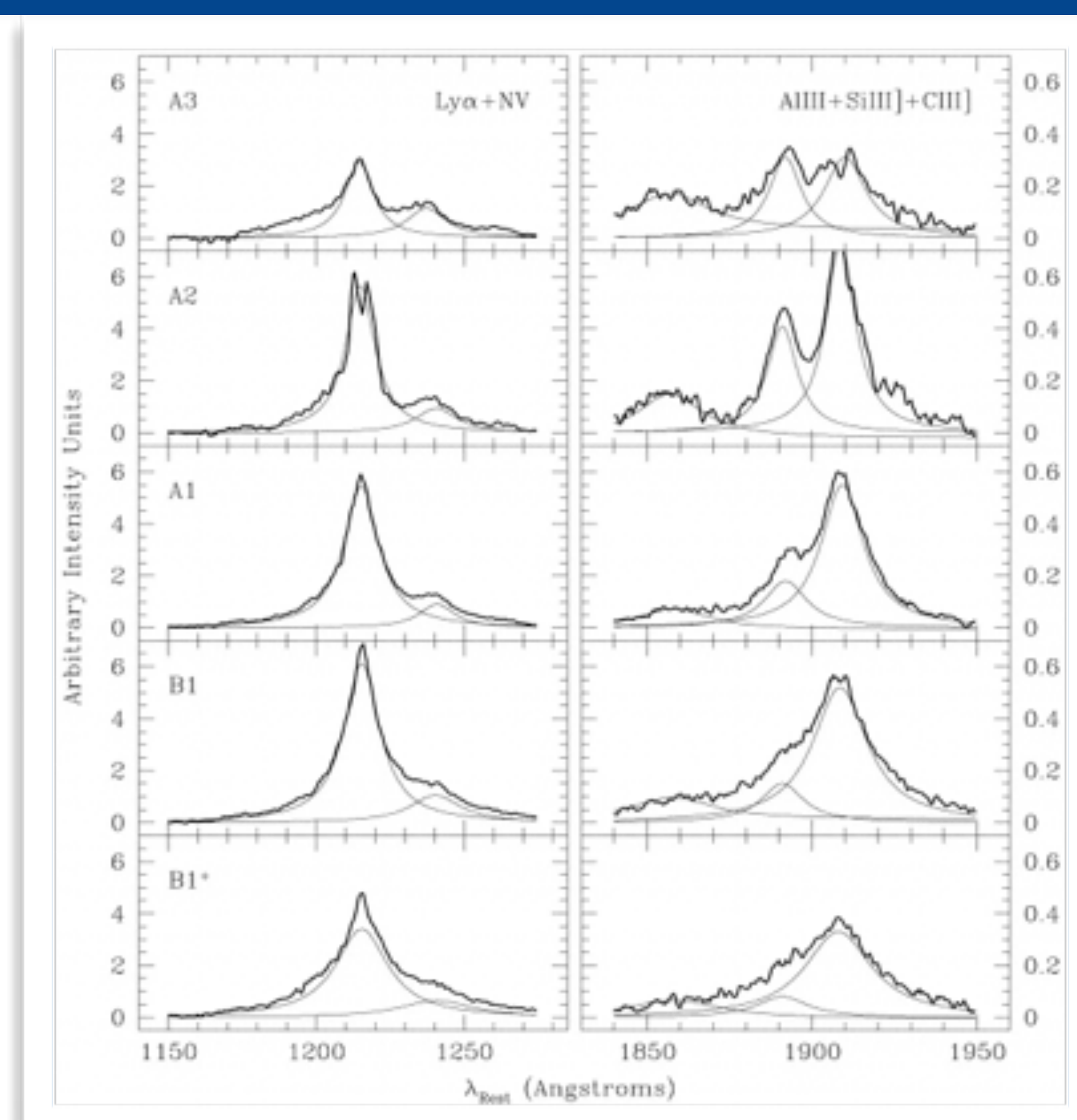

MS correlates: CIV emission line profile

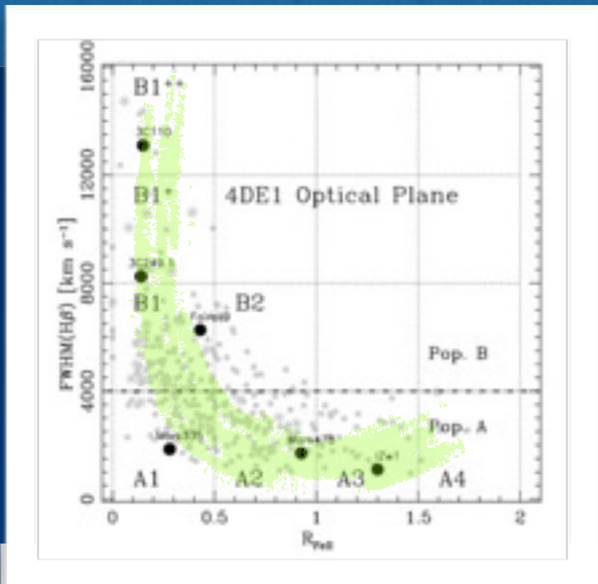

The CIVλ1549 line profile:
scaled Hβ from + excess blueshifted emission
virialized BLR symmetric + outflow/wind component

e.g., Leighly 2000, Bachev et al. 2004, Marziani et al. 2010; Denney et al. 2012

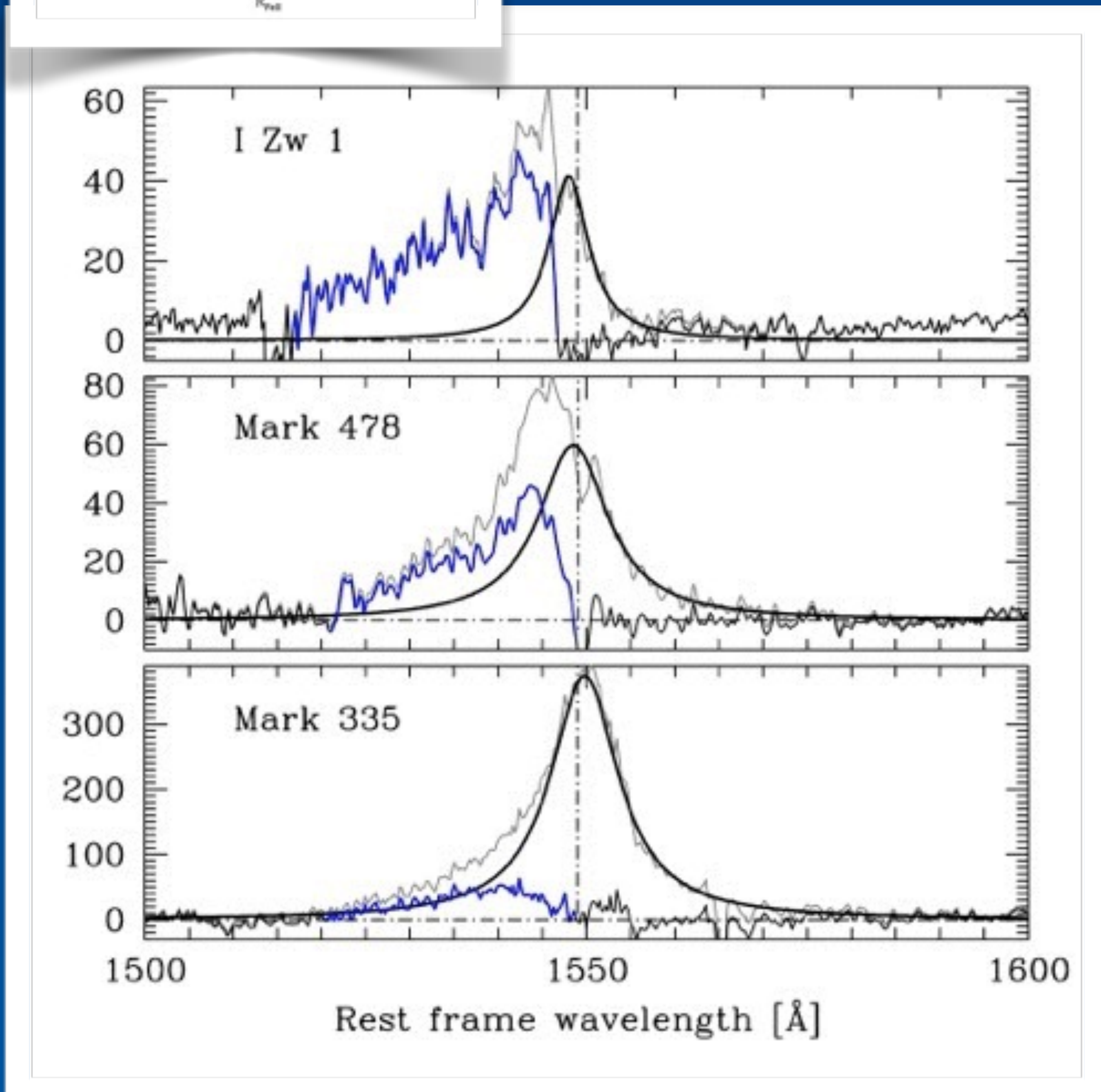

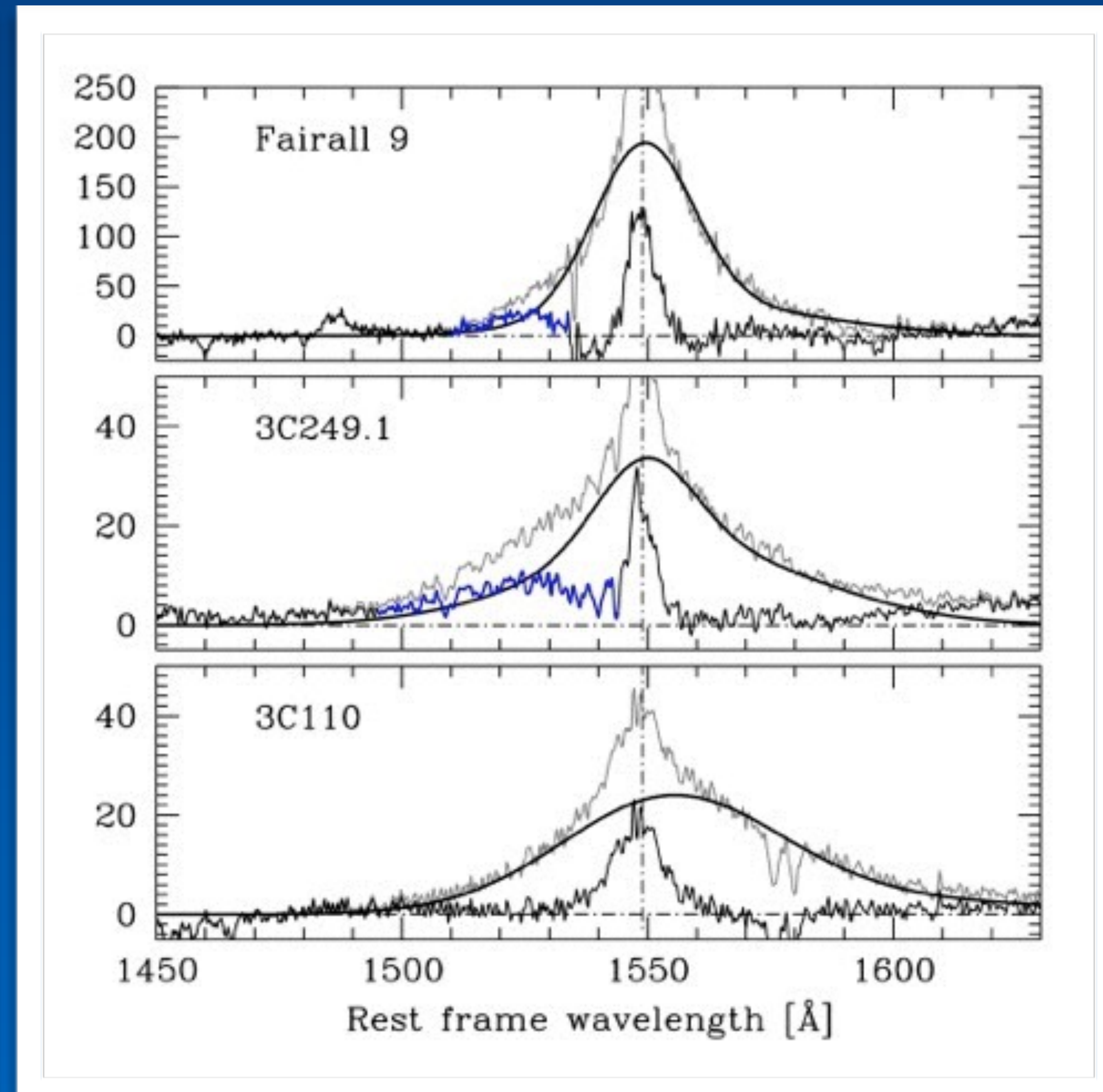

MS correlates: CIV centroid

Large shift of CIVλ1549 centroid at ½ along the main sequence are found for FWHM(Hβ)< 4000 km s^{-1}

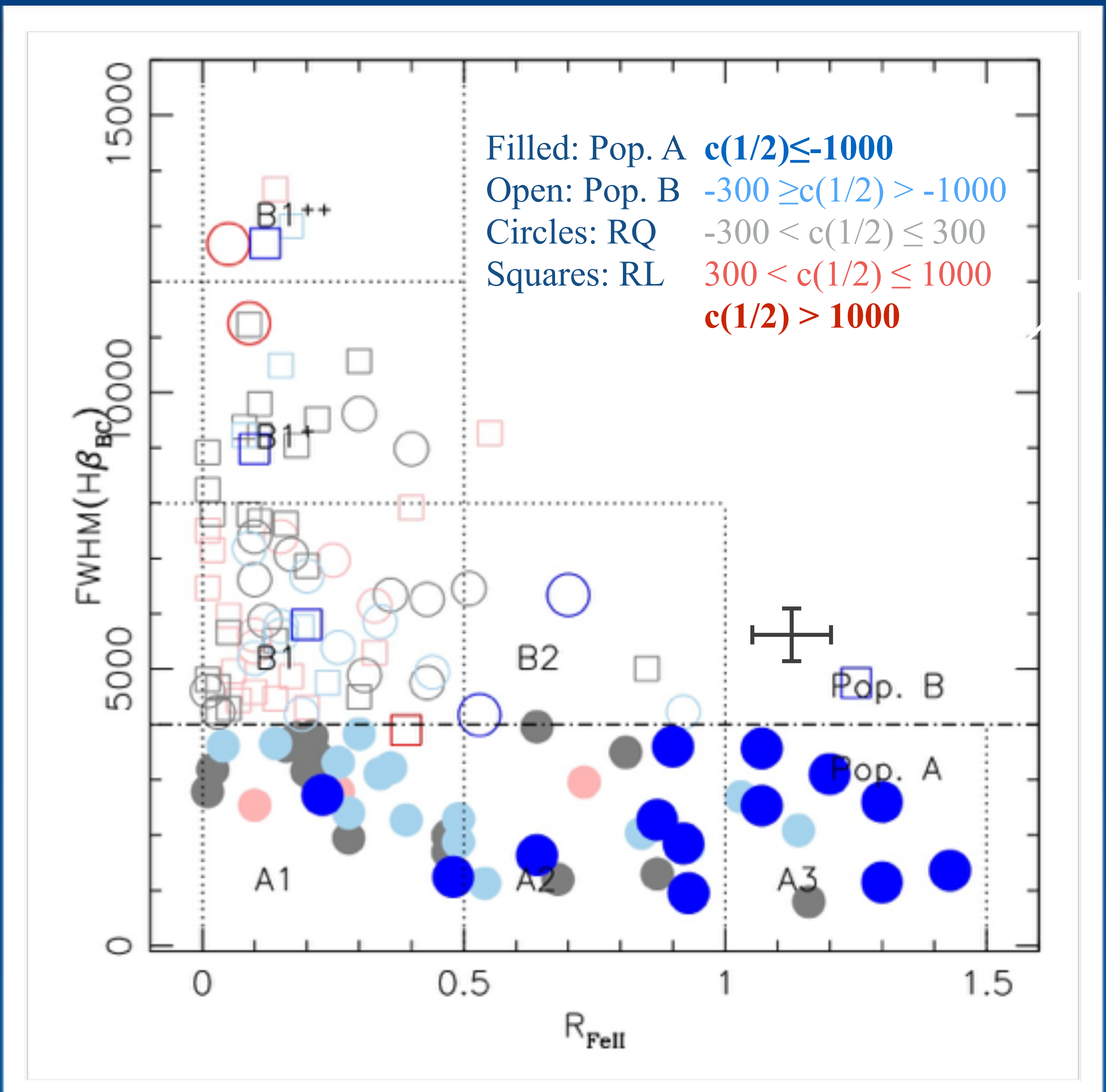

This result also reinforces the suggestion of a discontinuity at FWHM(Hβ) ≈ 4000 km s^{-1}

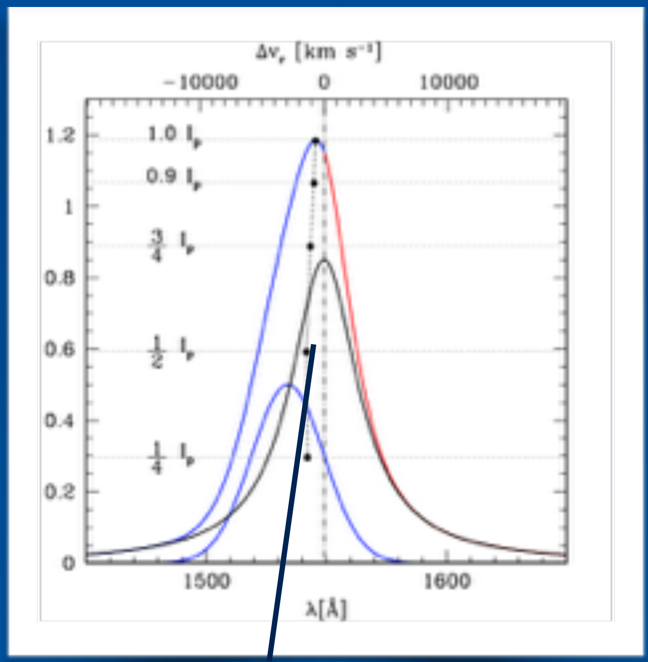

c(½) CIVλ1549

Marziani & Sulentic 2012; Sulentic et al. 2007; low *z* sample UV FOS data

MS correlates: CIV centroid

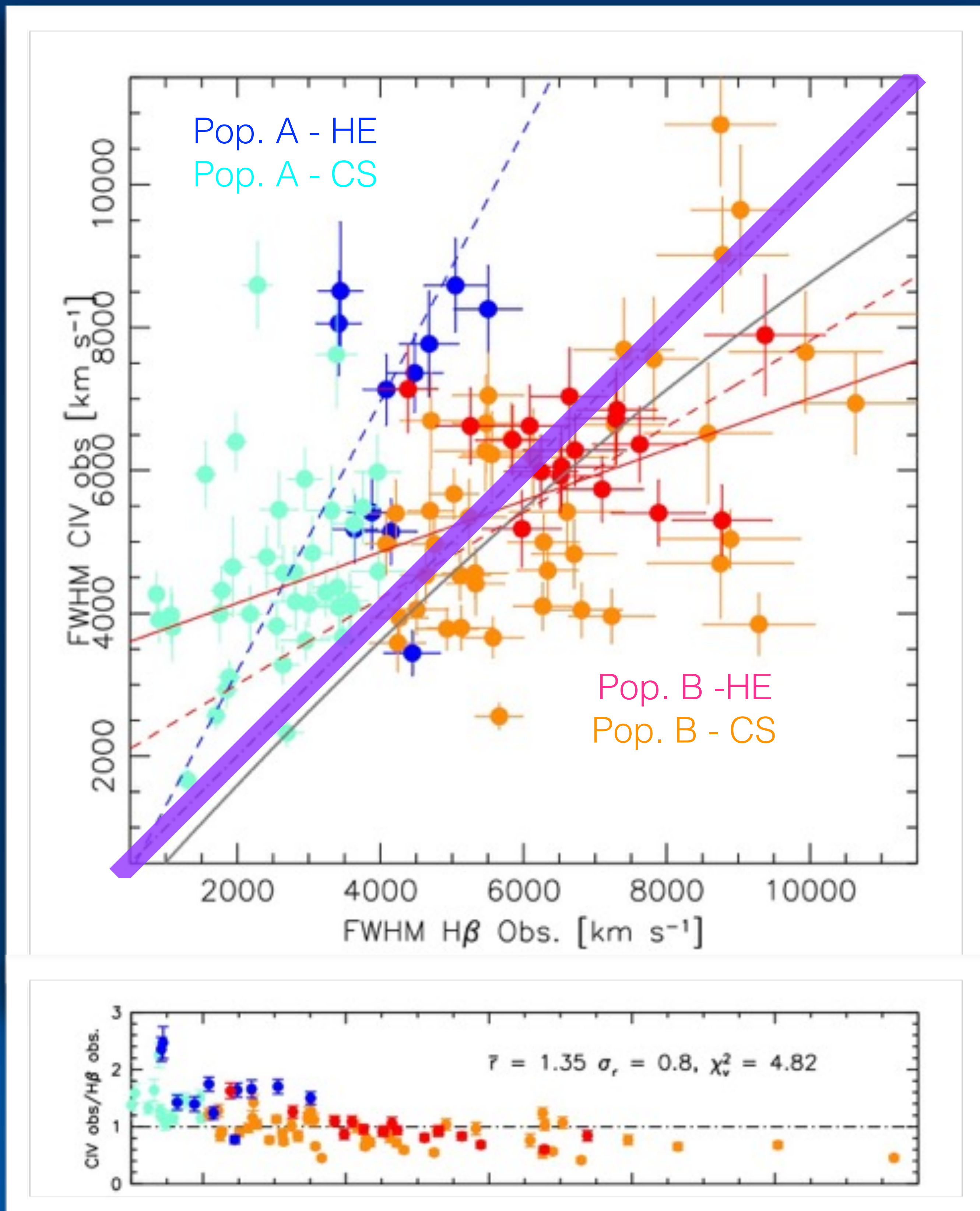

(Baskin & Laor 2005; Netzer et al. 2007; Sulentic et al. 2007; Ho et al. 2012; Trakhtenbrot & Netzer 2012)

The CIV line width is not usable as a virial broadening estimator

FWHM(CIVλ1549) for Pop.A sources is always above equality line with Hβ; large scatter for Pop. B.
The Park et al. 2013 scaling: consistent M_{BH} estimates only for Pop. A, assuming $M_{BH} \propto FWHM^{0.5}$

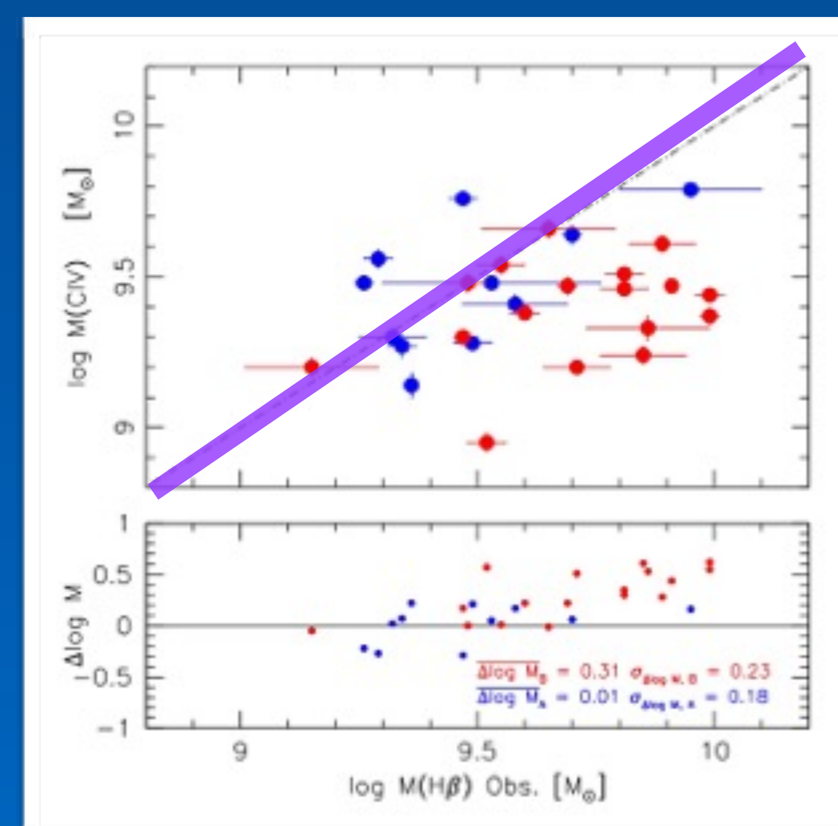

MS “correlates:” Eddington ratio

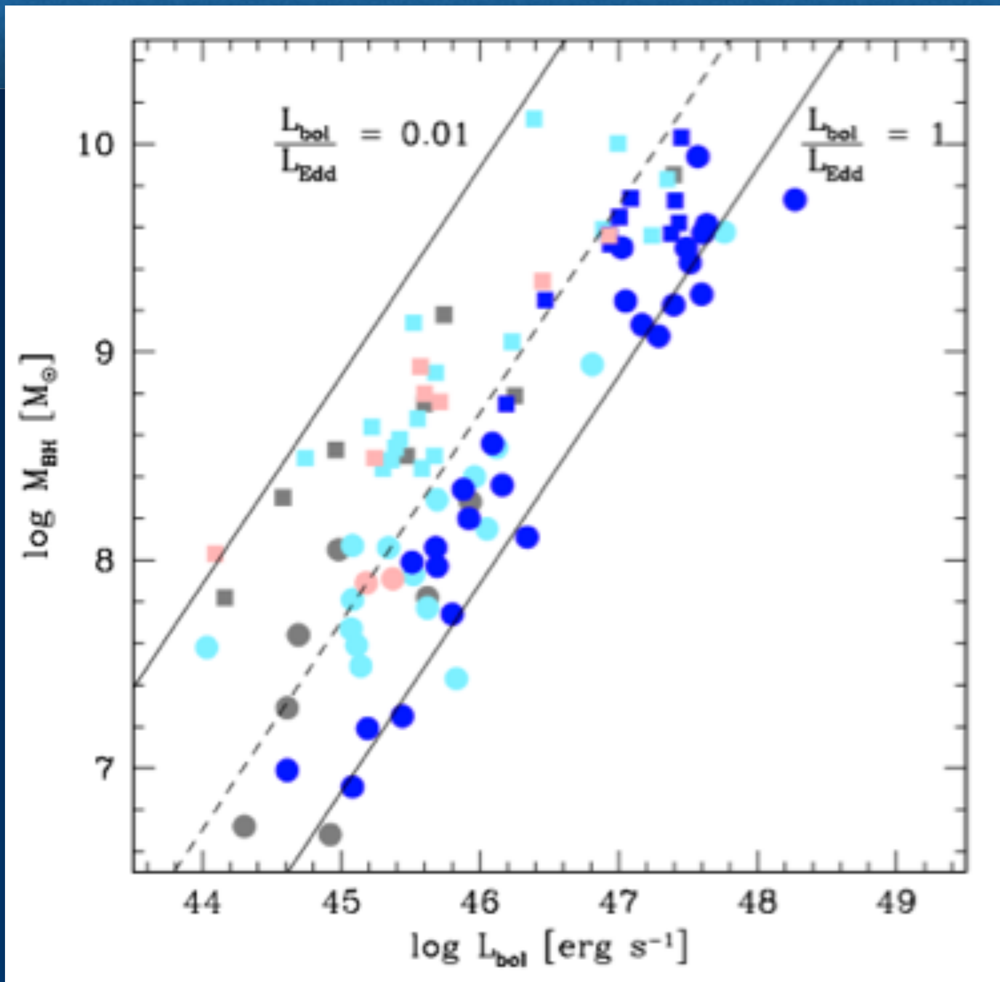

Largest CIVλ1549 blueshifts are observed at high L/L_{EDD} but not necessarily at high M_{BH} or high L

FOS + high L HE sample of 28 objects Sulentic et al. 2016, submitted

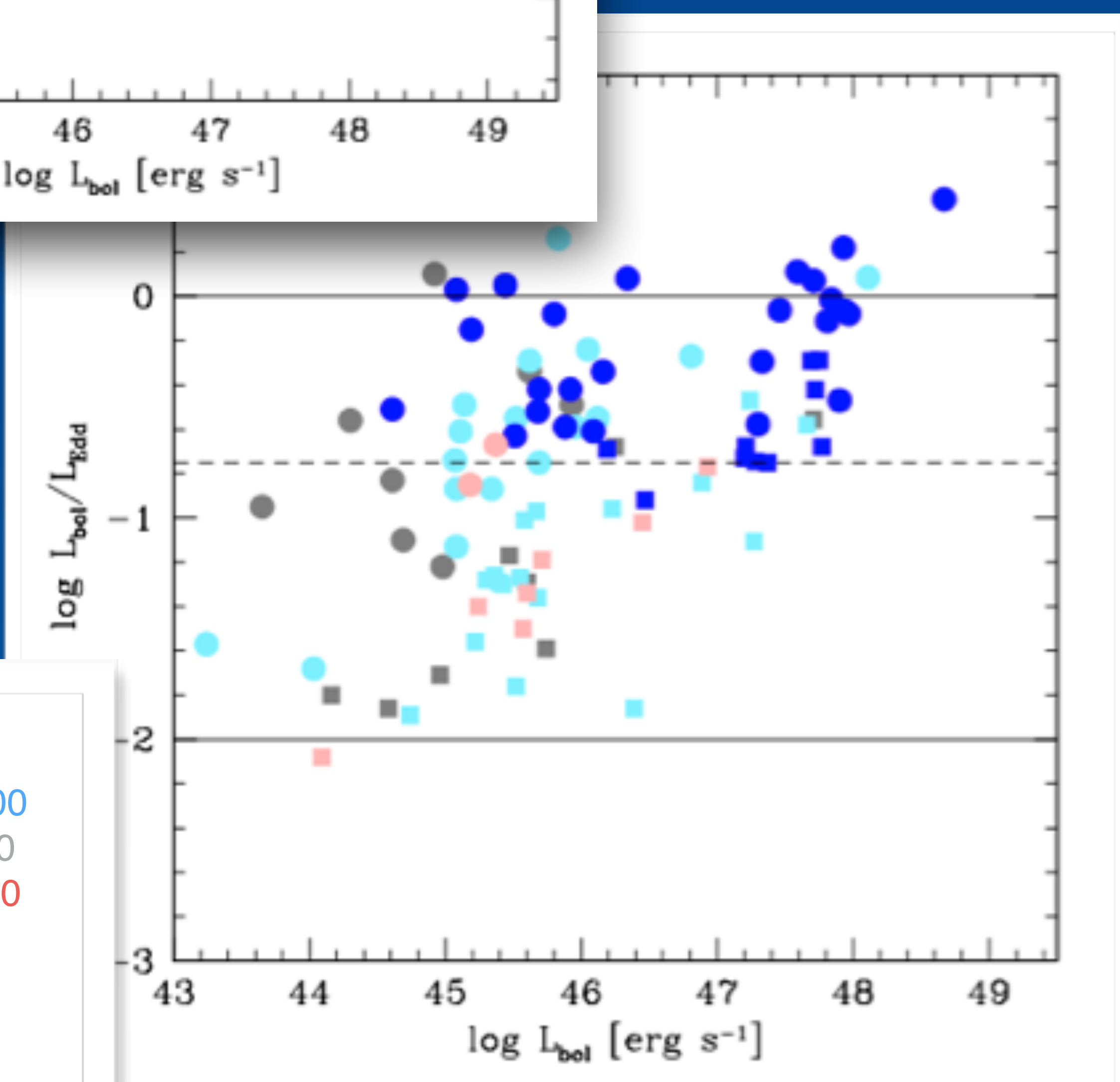

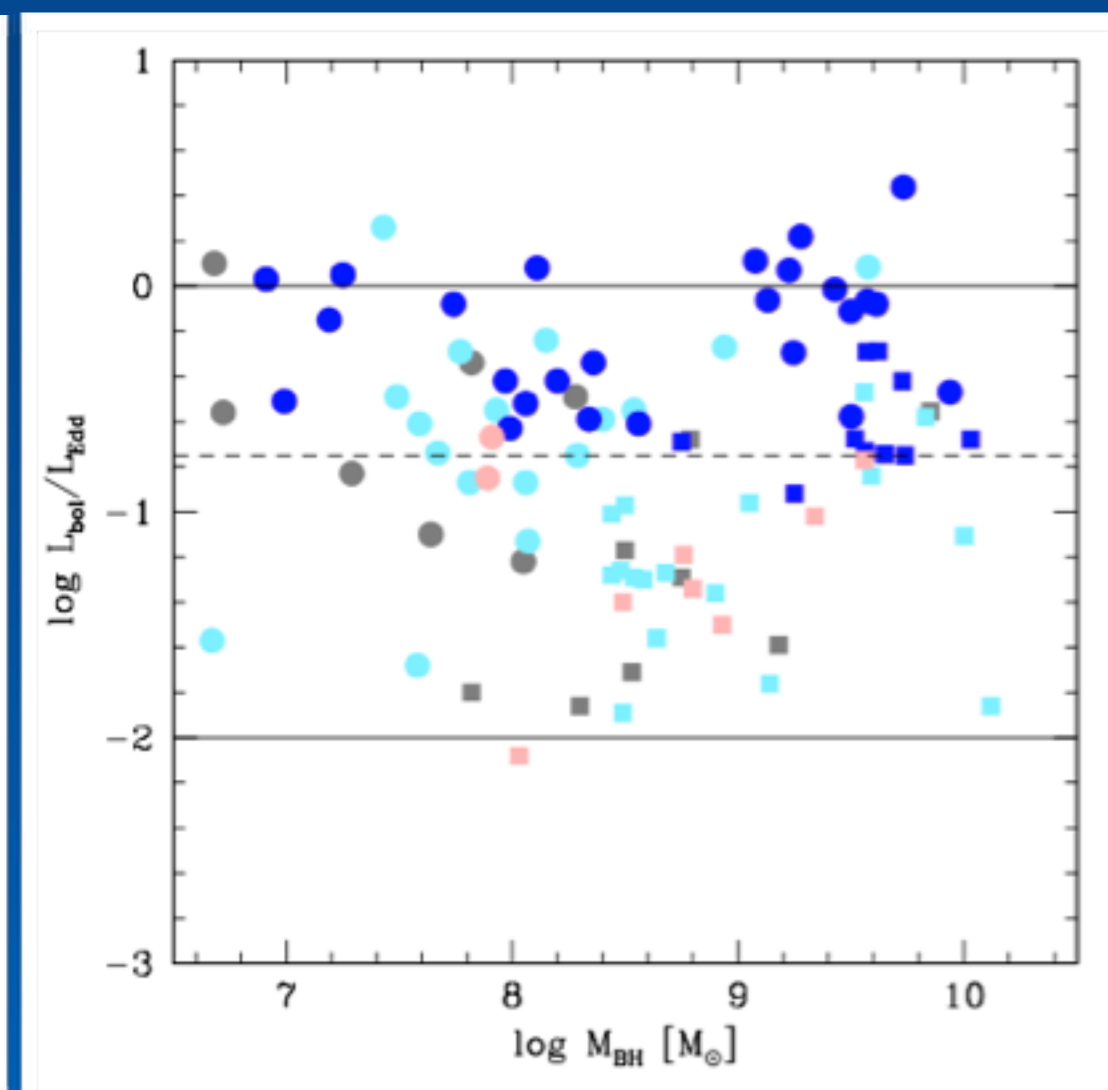

c(1/2)≤-1000
-300 ≥c(1/2) > -1000
-300 < c(1/2) ≤ 300
300 < c(1/2) ≤ 1000
c(1/2) > 1000
Circles: Pop. A
Squares: Pop. B

The MS: Governing physical parameters

MS: mainly a sequence of Eddington ratio

Ionization parameter U $\propto L/r_{BLR}^2 n \propto L^{1-2a}/n \propto L^{1-2a}/FWHM^{1.33}$

U ➜ $R_{FeII} \propto (L/M)^{-(1+x)} M^{-1}$ written as a function L/M_{BH} and M_{BH}, considering $r_{BLR} \propto L^a$, $n \propto FWHM^{1.33}$ (empirical relation)

Occupation reproduced assuming flattened geometry, FeII $\propto$ sec θ; $FWHM^2 \propto \delta v_{iso}^2 + \delta v_{rot}^2 \sin^2\theta$

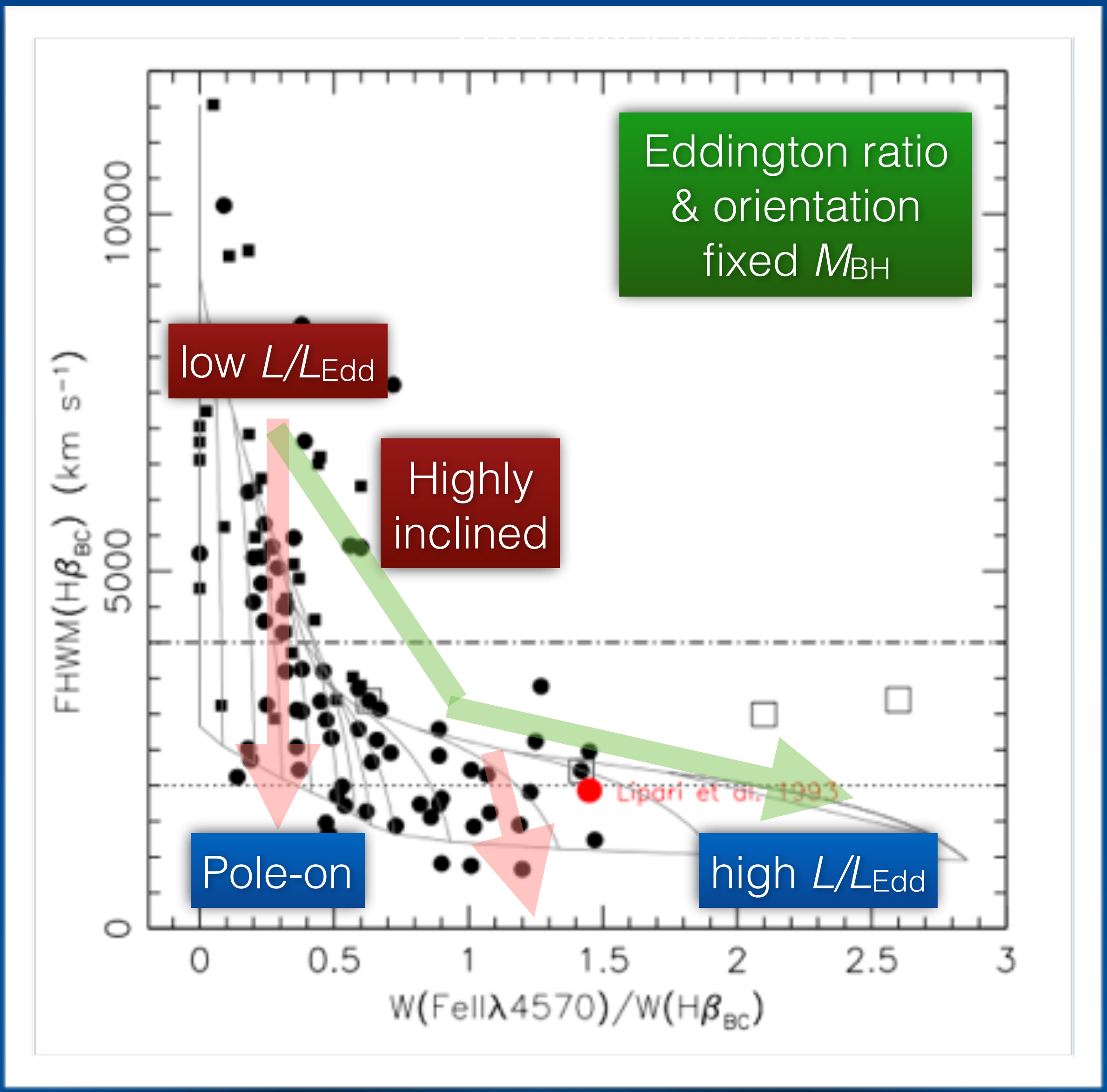

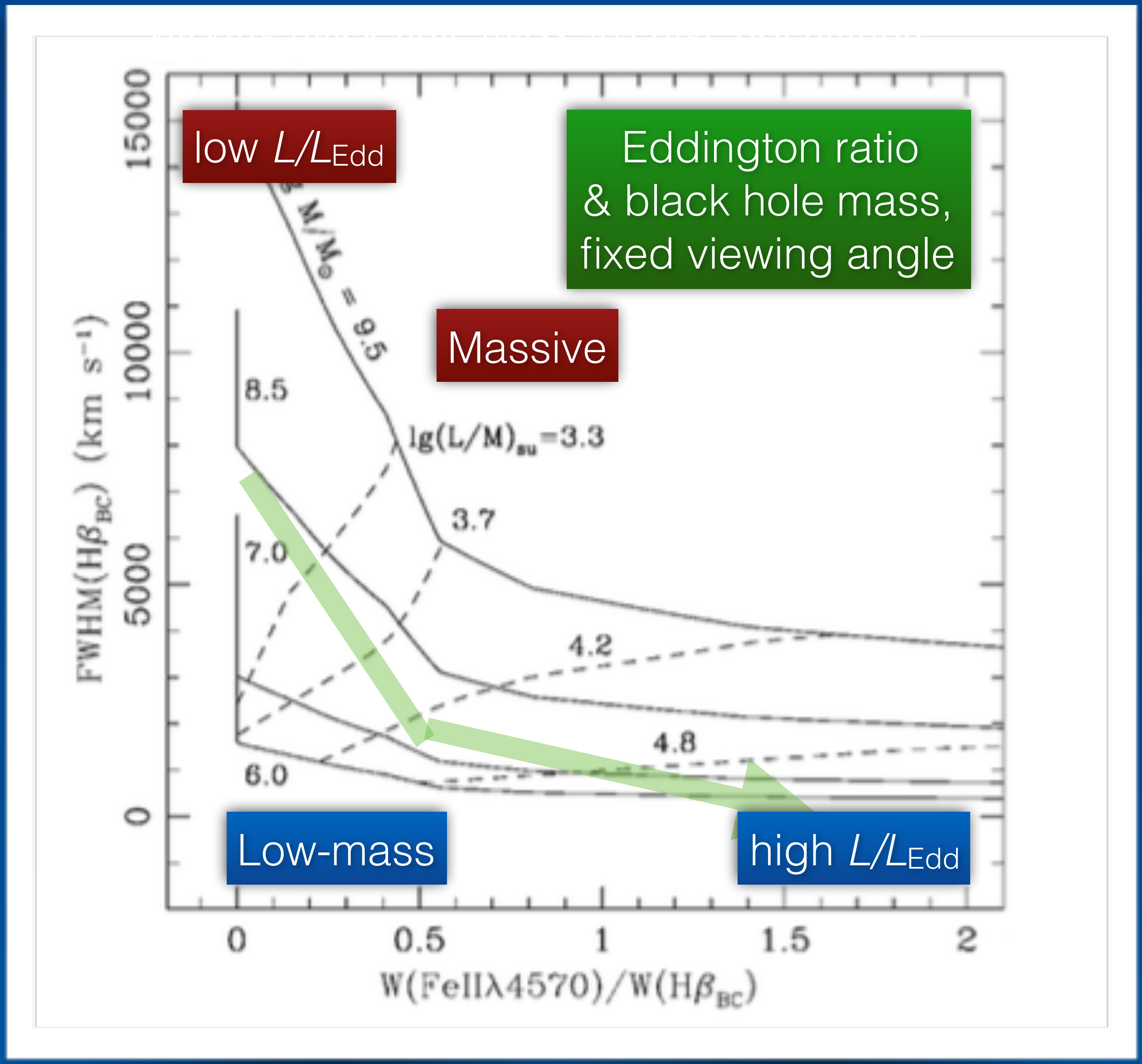

Marziani et al. 2001; Zamanov & Marziani 2002, cf. Shen & Ho 2014, Sun & Shen 2015

MS correlates: Two populations

Separation of Population A (FWHM Hβ<4000 km/s) and Population B(roader) sources.

At low *z*(<0.7) Pop. A: low M_{BH}, high L/L_{EDD}; Pop. B: high M_{BH}, low L/L_{EDD}; a reflection of the "downsizing" of nuclear activity

updated Table 1 of Sulentic et al. 2011

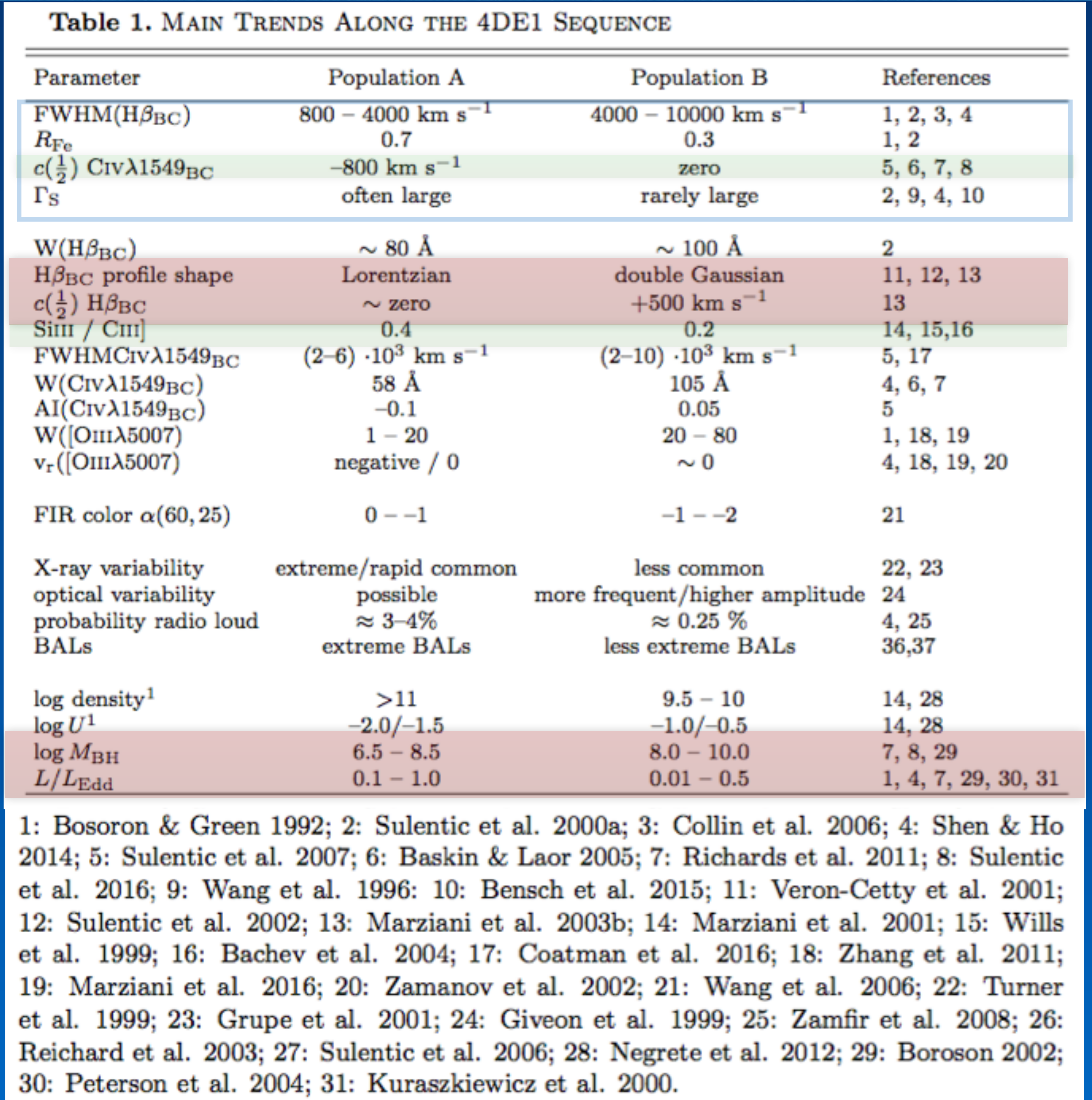

Table 1. MAIN TRENDS ALONG THE 4DE1 SEQUENCE

Parameter	Population A	Population B	References
FWHM($H\beta_{BC}$)	800 – 4000 km s^{-1}	4000 – 10000 km s^{-1}	1, 2, 3, 4
R_{Fe}	0.7	0.3	1, 2
$c(\frac{1}{2})$ CIVλ1549$_{BC}$	–800 km s^{-1}	zero	5, 6, 7, 8
Γ_S	often large	rarely large	2, 9, 4, 10
W($H\beta_{BC}$)	~ 80 Å	~ 100 Å	2
$H\beta_{BC}$ profile shape	Lorentzian	double Gaussian	11, 12, 13
$c(\frac{1}{2})$ $H\beta_{BC}$	~ zero	+500 km s^{-1}	13
SiIII / CIII]	0.4	0.2	14, 15,16
FWHMCIVλ1549$_{BC}$	(2–6) $\cdot 10^3$ km s^{-1}	(2–10) $\cdot 10^3$ km s^{-1}	5, 17
W(CIVλ1549$_{BC}$)	58 Å	105 Å	4, 6, 7
AI(CIVλ1549$_{BC}$)	–0.1	0.05	5
W([OIIIλ5007)	1 – 20	20 – 80	1, 18, 19
v_r([OIIIλ5007)	negative / 0	~ 0	4, 18, 19, 20
FIR color α(60, 25)	0 – –1	–1 – –2	21
X-ray variability	extreme/rapid common	less common	22, 23
optical variability	possible	more frequent/higher amplitude	24
probability radio loud	≈ 3–4%	≈ 0.25 %	4, 25
BALs	extreme BALs	less extreme BALs	36,37
log density[1]	>11	9.5 – 10	14, 28
log U^1	–2.0/–1.5	–1.0/–0.5	14, 28
log M_{BH}	6.5 – 8.5	8.0 – 10.0	7, 8, 29
L/L_{Edd}	0.1 – 1.0	0.01 – 0.5	1, 4, 7, 29, 30, 31

1: Bosoron & Green 1992; 2: Sulentic et al. 2000a; 3: Collin et al. 2006; 4: Shen & Ho 2014; 5: Sulentic et al. 2007; 6: Baskin & Laor 2005; 7: Richards et al. 2011; 8: Sulentic et al. 2016; 9: Wang et al. 1996: 10: Bensch et al. 2015; 11: Veron-Cetty et al. 2001; 12: Sulentic et al. 2002; 13: Marziani et al. 2003b; 14: Marziani et al. 2001; 15: Wills et al. 1999; 16: Bachev et al. 2004; 17: Coatman et al. 2016; 18: Zhang et al. 2011; 19: Marziani et al. 2016; 20: Zamanov et al. 2002; 21: Wang et al. 2006; 22: Turner et al. 1999; 23: Grupe et al. 2001; 24: Giveon et al. 1999; 25: Zamfir et al. 2008; 26: Reichard et al. 2003; 27: Sulentic et al. 2006; 28: Negrete et al. 2012; 29: Boroson 2002; 30: Peterson et al. 2004; 31: Kuraszkiewicz et al. 2000.

Pop. A/B transition: geometrically thick/thin disk?

Not drawn to scale

Abramowicz et al. 1988, Shakura & Sunyaev 1973

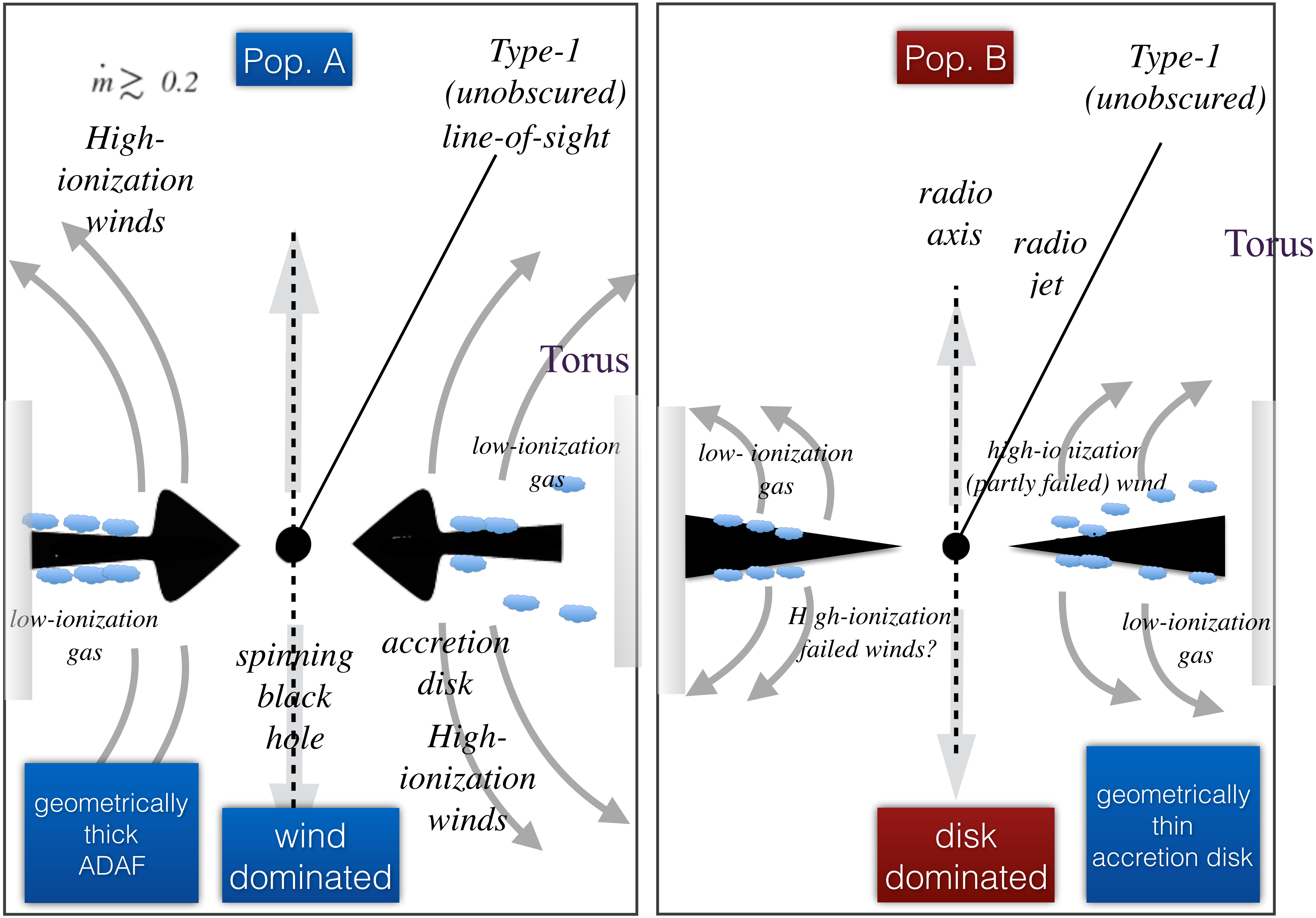

The MS: The MS “tip”

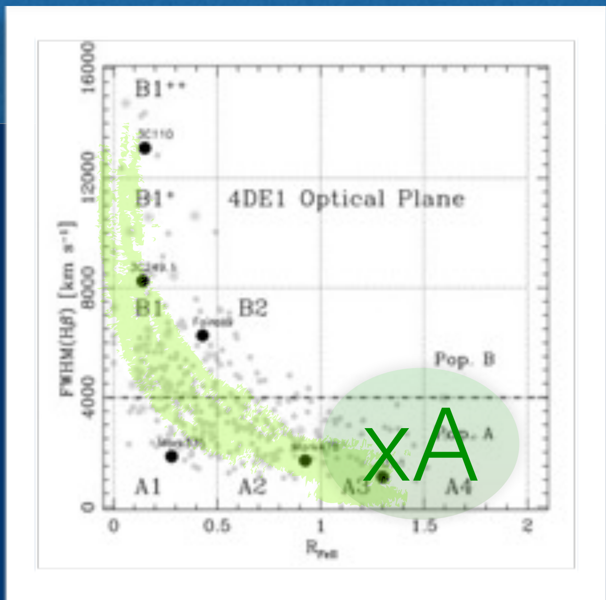

Extreme Pop. A quasars (xA)

Simple selection criteria from diagnostic line ratios

1) R_{FeII} = FeIIλ4570 blend/Hβ > 1.0

2) UV AlIII λ1860/SiIII]λ1892>0.5 & SiIII]λ1892/ CIII]λ1909>1

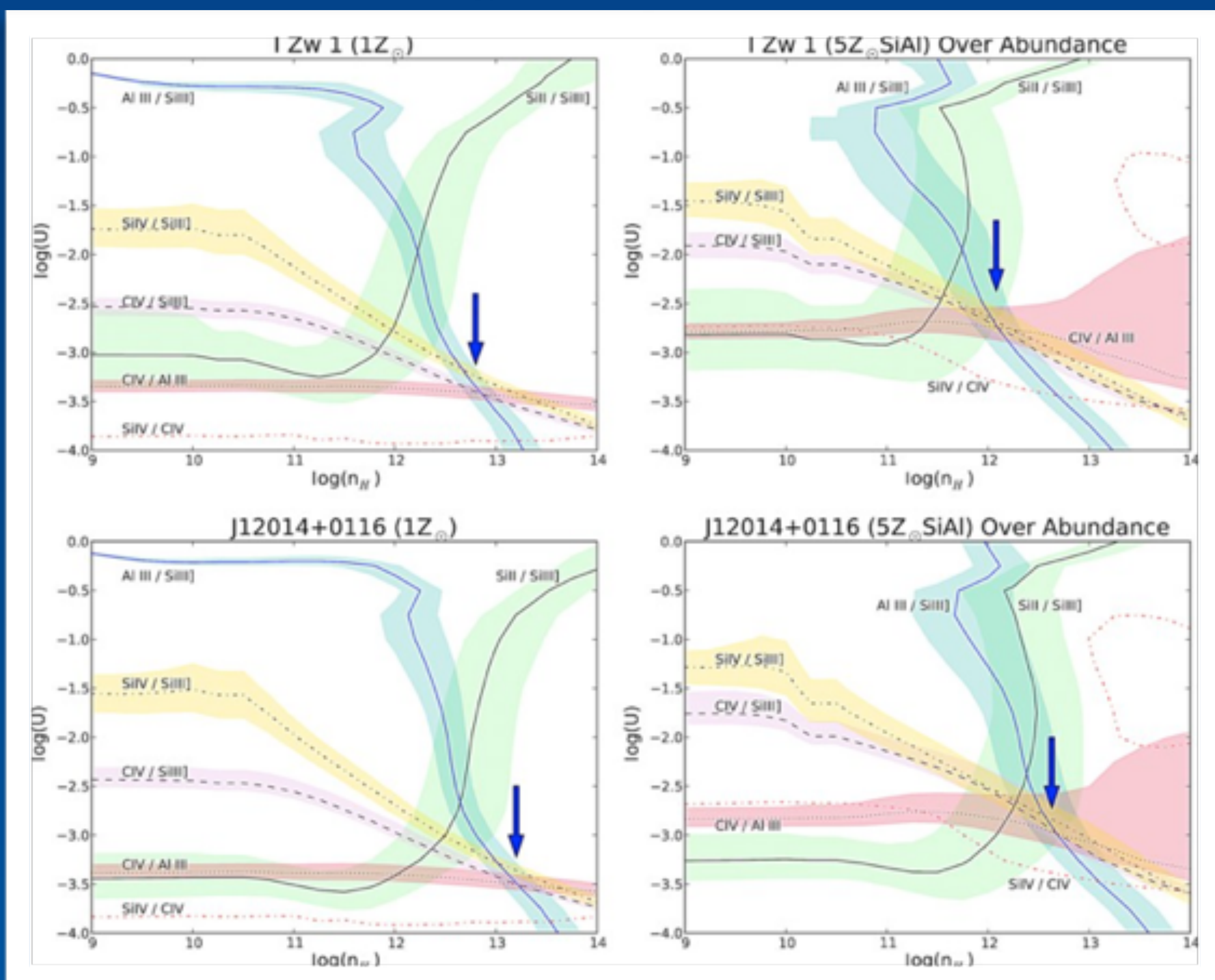

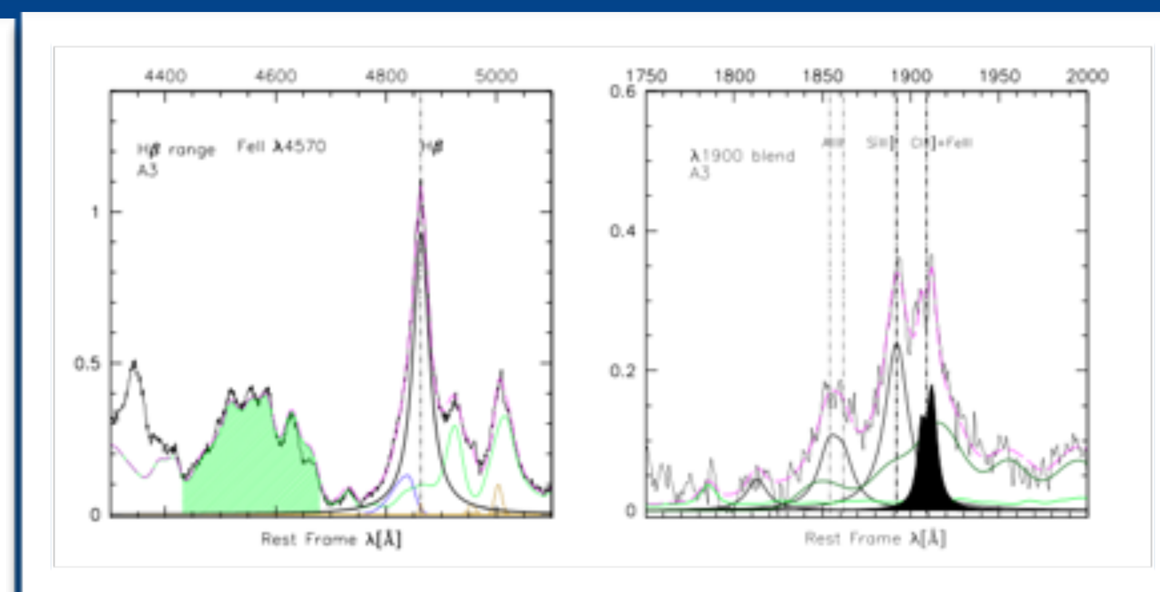

Extreme, well defined-values for density (high), ionization (high) and metallicity (high): Some xA are weak lined quasars

Plane ionization parameter versus density (Negrete et al. 2012)

Extreme Pop. A (xA) sources: associated with a tight distribution of Eddington ratio, in agreement with theoretical expectations

It is then possible to retrieve the quasar luminosity if the virial mass is known

$$\frac{L}{L_{\mathrm{Edd}}} = \eta \qquad L = \eta L_{\mathrm{Edd}} = \mathrm{const}\,\eta M_{\mathrm{BH}}$$

$$L \approx 7.8\ 10^{44} \frac{\eta_1^2 \kappa_{0.5} f_2^2}{\bar{\nu}_{\mathrm{i}2.42\ 10^{16}}} \frac{1}{(nU)_{9.6}} v_{1000}^4 \quad \mathrm{erg\ s^{-1}}$$

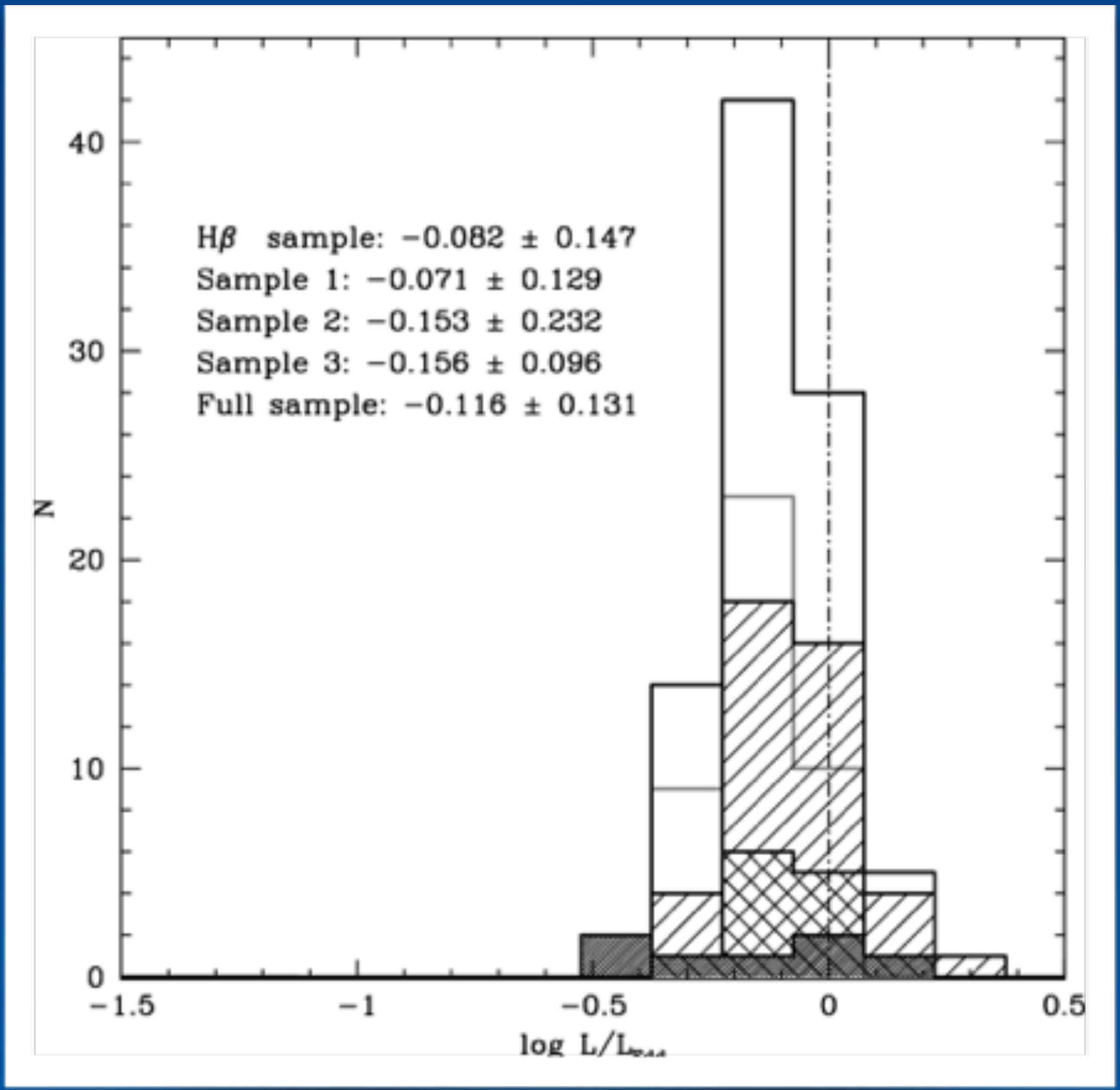

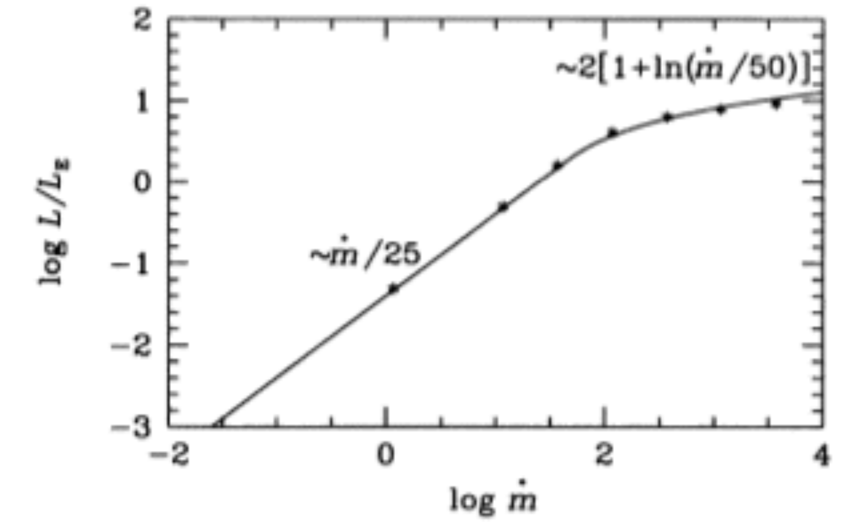

Fig. 2. Disk luminosity as a function of ṁ. The asterisks denote the calculated luminosities, whereas the solid line shows the fitting formula (8). It is clear that an increase in L is suppressed at $L > 2L_{\mathrm{E}}$.

Wang et al. 2003 Mineshige et al. 2000

Conclusion

The MS is most likely a sequence of L/L_{Edd} . An accretion mode change may be associated with a critical $L/L_{Edd} \sim 0.2$, leading to two quasars populations: A (wind-dominated), and B (disk dominated).

(preliminary)

xA quasars at the high R_{FeII} end of the MS show a small scatter in L/L_{Edd} and may be suitable as Eddington standard candles.

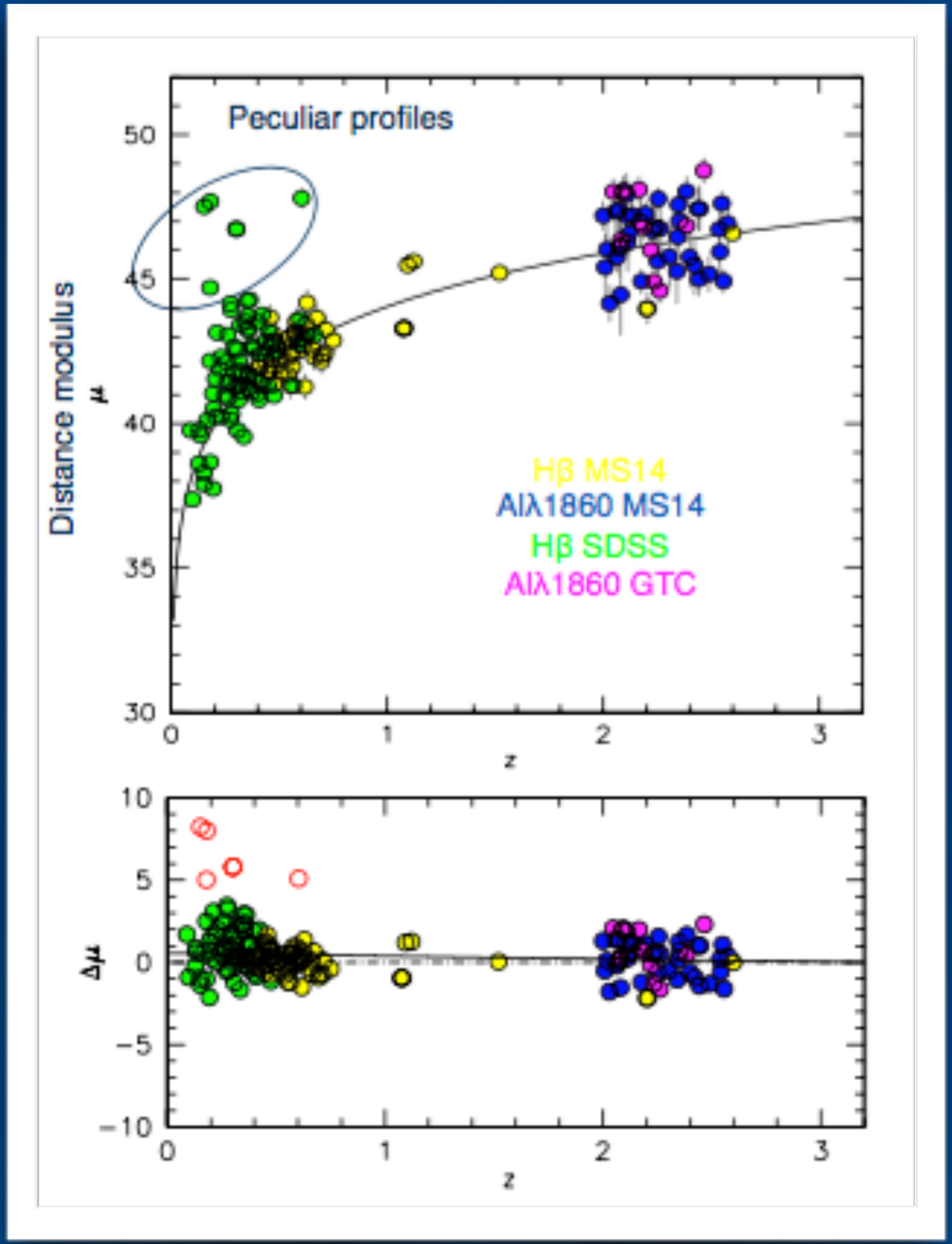

Huge quasar samples ($\sim 10^5$ sources) are now available from major surveys completed and in progress (LBQS, SDSS, 2dF, BOSS). The E1 approach offers contextualization for internal line shifts, profiles of spectral lines, as well as many multifrequency spectrophotometric measures.